

Resonant photoemission study of $\text{Ba}_{1-x}\text{K}_x\text{BiO}_3$ single crystals

H. Nylén, G. Chiaia,* A. A. Zakharov, M. Qvarford, and I. Lindau

Department of Synchrotron Radiation Research, Institute of Physics, Lund University, Box 118, S-221 00 Lund, Sweden

V. G. Nazin, M. B. Tsetlin, and M. N. Mikheeva

Russian Research Center "Kurchatov Institute," Kurchatov square 1, 123182 Moscow, Russia

S. N. Barilo and S. V. Shiryayev

Institute of Solid State Physics and Semiconductors, 220072, Minsk, Belorussia

(Received 12 December 1996)

Single crystals of superconducting $\text{Ba}_{0.6}\text{K}_{0.4}\text{BiO}_3$ and semiconducting $\text{Ba}_{0.9}\text{K}_{0.1}\text{BiO}_3$ have been studied by resonant photoemission. In the photon energy range 14–25 eV, a valence-band feature with a binding energy around 2.6 eV becomes enhanced at the photon energies 16, 19, and 22.5 eV. In order to identify this possibly resonating feature, valence-band photoemission spectra were also measured at photon energies (90–120 eV) around the excitation threshold of the Ba 4*d* core level. A comparison between the results obtained at these different photon energy regions suggests that the valence-band enhancements at 16 and 19 eV can be assigned to resonating Ba states, while the comparatively weaker enhancement at 22.5 eV is consistent with both a Ba and/or an O photoemission resonance. The results also indicate Ba states close to the Fermi level. [S0163-1829(97)03130-5]

I. INTRODUCTION

Since the discovery of high-temperature superconductivity in the $\text{Ba}_{1-x}\text{K}_x\text{BiO}_3$ perovskite by Mattheiss, Gyorgy, and Johnson,¹ investigations of its electronic structure have been of fundamental interest. $\text{Ba}_{1-x}\text{K}_x\text{BiO}_3$ exhibits the highest T_c (~ 30 K) at a potassium content of $x=0.4$ for which it has a cubic structure while for $x=0.1$, this compound shows semiconducting properties. Various attempts to calculate the band structure and associated partial density of states (DOS) of $\text{Ba}_{1-x}\text{K}_x\text{BiO}_3$ by applying different approximations, have been reported by a number of authors.²⁻⁷ Mattheiss and Hamann⁴ did the calculation on BaBiO_3 and ordered $\text{Ba}_{0.5}\text{K}_{0.5}\text{BiO}_3$ using the linear augmented plane-wave (LAPW) method. Hamada *et al.*⁵ performed the LAPW calculation on cubic BaBiO_3 and treated the potassium alloying as a rigid band shift. Papaconstantopoulos *et al.*⁶ made separate APW calculations on both BaBiO_3 and KBiO_3 and fitted the results to a tight-binding Hamiltonian. The DOS for disordered $\text{Ba}_{0.6}\text{K}_{0.4}\text{BiO}_3$ were then calculated using the coherent potential approach. All calculations show that the main contribution to the valence band consists of O states and smaller fractions of Ba, K, and broadly distributed Bi states. For cubic $\text{Ba}_{1-x}\text{K}_x\text{BiO}_3$, corresponding to the metallic phase, the calculations predict that a Bi-O band crosses the Fermi level. From these calculations, the assignments of valence-band features in photoemission spectra are facilitated.

In previous photoemission studies of BaBiO_3 and $\text{Ba}_{0.6}\text{K}_{0.4}\text{BiO}_3$, a broad enhancement in constant initial state plots of the valence band has been reported for photon energies (PE) between 19 and 22 eV.⁸⁻¹⁰ This enhancement has been suggested to be due to a O 2*p* resonance corresponding to the O 2*s*-2*p* absorption threshold. However, inverse pho-

toemission shows no O 2*s*-2*p* resonant enhancement for $\text{Ba}_{1-x}\text{K}_x\text{BiO}_3$.¹¹

In this paper, we present results from resonant photoemission measurements performed on single crystals of superconducting $\text{Ba}_{0.6}\text{K}_{0.4}\text{BiO}_3$ and semiconducting $\text{Ba}_{0.9}\text{K}_{0.1}\text{BiO}_3$. The photon energy ranges were chosen to match absorption thresholds of different core levels (Ba 4*d*, O 2*s*, K 3*p*, and Ba 5*p*). The valence-band data showed pronounced intensity modulations as the PE was changed in the range 14–25 eV and exhibited maximum enhancements at 16, 19, and 22.5 eV. From the analysis in Sec. III, it is concluded that the enhancements at the first two photon energies (16 and 19 eV) can be attributed to photoemission resonances of Ba valence states, while the weaker 22.5 eV resonance can be interpreted as being Ba and/or O related.

II. EXPERIMENTAL

Photoelectron spectroscopy (PES) of the valence band of freshly cleaved single crystals of superconducting $\text{Ba}_{0.6}\text{K}_{0.4}\text{BiO}_3$ and semiconducting $\text{Ba}_{0.9}\text{K}_{0.1}\text{BiO}_3$ has been performed at the national synchrotron radiation laboratory MAX-lab in Lund, Sweden. The growth and characterization of the $\text{Ba}_{0.6}\text{K}_{0.4}\text{BiO}_3$ and $\text{Ba}_{0.9}\text{K}_{0.1}\text{BiO}_3$ single crystals are described elsewhere.¹² The crystals were glued with silver epoxy to copper sample holders and cleaved *in situ* at a pressure of about 10^{-10} torr. Due to the low surface stability of $\text{Ba}_{1-x}\text{K}_x\text{BiO}_3$, the samples were cooled with liquid nitrogen during fracturing and measurements. The size of the cleaved sample surfaces was about 3×3 mm². The resulting (100) surfaces were rough and brown for the $x=0.1$ composition, while blue for $x=0.4$. The potassium and/or oxygen concentration at the surface seemed to vary among the samples because variations of the spectral intensity near the Fermi level were seen in some cases between different samples

with the same nominal composition. Also, some of the semiconducting samples showed insulating properties when cooled with liquid nitrogen which resulted in charging of these samples during measurements. The charging effect occurred on a large time scale, typically 1 eV shift after 3 h of measurements which means that the shape of the valence band was not altered during acquisition of each spectrum. Although the structural phase diagram for $\text{Ba}_{1-x}\text{K}_x\text{BiO}_3$ from Pei *et al.*¹³ shows that the $x=0.1$ compound is located at the transition between the monoclinic and orthorhombic phases at this temperature, we believe that the crucial differences leading to different charging properties among the semiconducting samples at liquid-nitrogen temperature are deviations in the homogeneity, in the contents of potassium and oxygen and/or crystal defects among the samples.

The measurements at low photon energies took place at beamline (BL) 52 (Ref. 14) which is equipped with a normal incidence monochromator and an angle-resolved 50-mm mean radius hemispherical electron energy analyzer mounted on a goniometer. The total-energy resolution in these measurements was about 200 meV. The high PE (90–125 eV) spectra were recorded at BL 22 which has a modified SX-700 plane grating monochromator¹⁵ and a 200-mm mean radius hemispherical electron energy analyzer with a multichannel-plate detector.¹⁶ The photon flux was determined by measuring the photocurrent from a gold mesh, taking into account the photoelectric yield of gold.^{17,18} The binding energies were calibrated with respect to the Fermi edge of a gold reference sample. All spectra presented, except when explicitly noted, were measured at normal emission.

III. RESULTS AND DISCUSSION

Valence-band photoemission spectra measured at different photon energies in the range 14.5–23 eV are shown in Fig. 1 for the superconductor $\text{Ba}_{0.6}\text{K}_{0.4}\text{BiO}_3$. In this photon energy region, several intensity modulations are seen in the valence band. In order to achieve an intensity profile of the valence band, constant initial state (CIS) plots extracted from the spectra in Fig. 1 around resolved structures in the valence band, i.e., at the binding energies (E_b) 2.6, 3.8, and 6.3 eV, are shown in Fig. 2. For information regarding the influence from the inelastic background of the most enhanced feature at 2.6 eV E_b on the CIS curves at 3.8 and 6.3 eV, a CIS plot of the featureless region at 5.2 eV (the dip in the valence band), is also shown. A binding energy window of 0.3 eV was used in order to minimize the influence of statistical fluctuations. The photon energies, for which the spectra discussed below are recorded, are labeled $a-i$ in the CIS plot. From the CIS curves, three different intensity maximums can be seen in the valence band which is most enhanced at 19 and 16 eV PE (b and e) and has a smaller intensity maximum at 22.5 eV (h). The most pronounced feature is located at 2.6 eV binding energy while the features at 3.8 and 6.3 eV have weaker intensity modulations. The 5.2 eV E_b CIS curve is slightly less modulated than the 3.8 and 6.3 eV curves which suggests that the latter two are not only affected by intensity variations of inelastically scattered electrons. To obtain information regarding the nature of the intensity modulations, a spectrum subtraction procedure has been ap-

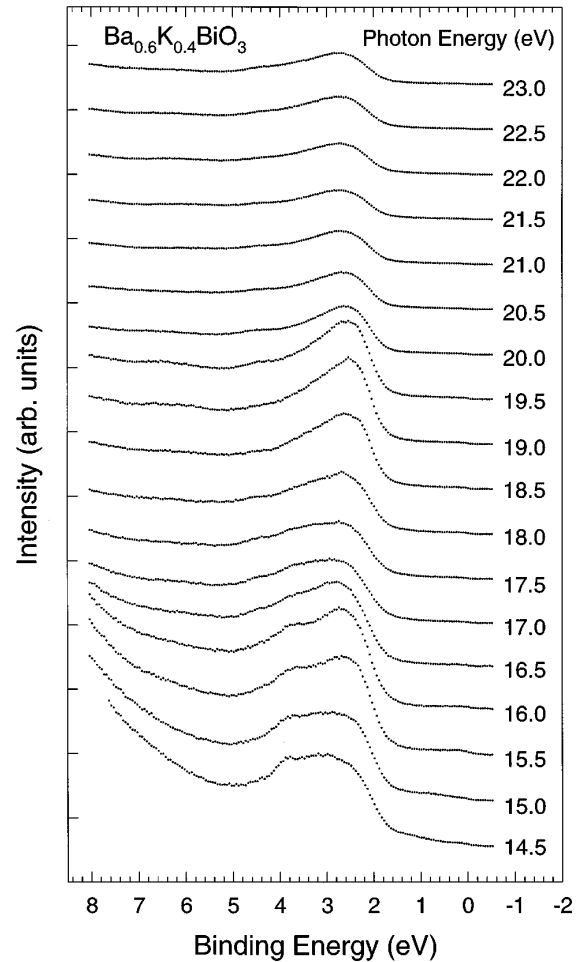


FIG. 1. Valence-band photoemission spectra of superconducting $\text{Ba}_{0.6}\text{K}_{0.4}\text{BiO}_3$ measured at different photon energies in the range 14.5–23 eV. The spectra are normalized with respect to the photon flux.

plied. The difference spectra are shown in Fig. 3 and are labeled 1–3 corresponding to the enhancements seen in the valence band at photon energies of 16, 19, and 22.5 eV, respectively. They were obtained by subtracting the mean of two spectra, one from each photon energy side of the maximum, from the spectrum displaying the largest enhancement. For clarity, the difference spectra are also denoted in terms of the subtraction procedure used, e.g., $b-(a+c)/2$ for spectrum 1. By this method of subtraction, the effect from changes in the atomic cross sections is minimized. The difference spectra 1 and 2 show a similar peaked structure around 2.5 eV binding energy with a full width at half maximum (FWHM) of about 1.2 eV. Spectrum 2 has the maximum main peak intensity together with a small structure at 6.3 eV E_b while spectrum 1 has a comparatively intense region ranging from 3.3 to 7.5 eV, to some extent caused by the different influence from the inelastic tail among the valence-band spectra a , b , and c .¹⁹ The main peak in difference spectrum 3 is much less intense and broader (FWHM ≈ 2 eV, which is about the same as the valence band) than in spectra 1 and 2, followed by a weaker structure at about 6.7 eV.

There are two possible explanations for the intensity variations in the valence band which need to be considered:

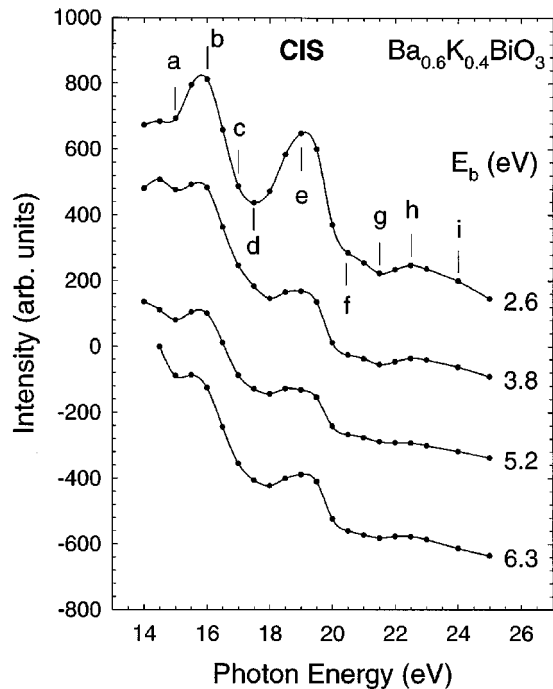


FIG. 2. Valence-band CIS plots of $Ba_{0.6}K_{0.4}BiO_3$ at binding energies 2.6, 3.8, 5.2, and 6.3 eV, extracted from the spectra in Fig. 1. An arbitrary offset is applied to each CIS curve while the absolute intensity scales with the top curve.

band-structure effects and photoemission resonances, the latter being due to the interference between the direct photoemission and an autoionization channel at a core-level

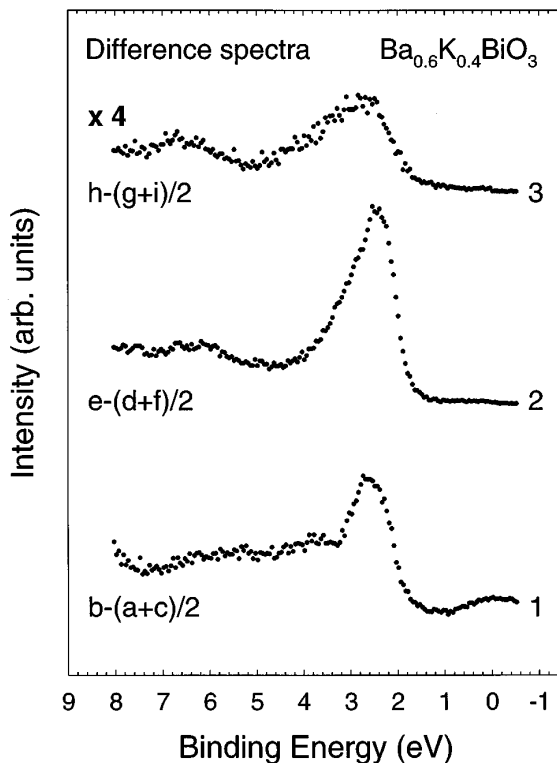


FIG. 3. Difference spectra 1, 2, and 3 corresponding to the enhancements b , e , and h in Fig. 2, respectively. The calculation procedure is described in the text.

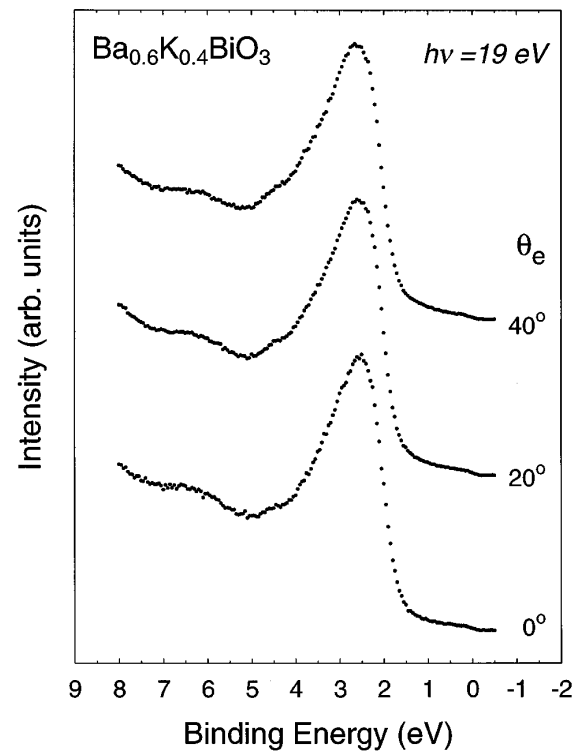


FIG. 4. Valence-band photoemission spectra of $Ba_{0.6}K_{0.4}BiO_3$ measured at a photon energy of 19 eV for the different emission angles 0° , 20° , and 40° .

threshold which lead to the same final state.²⁰ The former explanation, that the intensity variations would arise because of the probing of, e.g., high-symmetry points in the band structure, was investigated by measuring valence-band spectra at different emission angles. These spectra, measured at 19 eV PE in order to follow the behavior of the most pronounced enhancement at 2.6 eV E_b , are shown in Fig. 4. As seen in this figure, no clear changes in the spectral shape occurred when the emission angle was changed suggesting that the intensity modulation around 19 eV PE is not due to band-structure effects.²¹ It should also be noted that the calculated band structure in the Γ - X direction, i.e., the direction probed in the normal emission series in Fig. 1, exhibits rather flat bands around 3 eV.²⁻⁷ Thus, the valence-band modulation at 19 eV PE is more likely to be understood as a photoemission resonance. The same conclusion was reached for the modulations around 16 and 22.5 eV PE because of the negligible angular dependency of the valence-band spectral shape (not shown).

In Fig. 5, a comparison is made between the valence bands of the superconductor $Ba_{0.6}K_{0.4}BiO_3$ and the semiconductor $Ba_{0.9}K_{0.1}BiO_3$ at photon energies corresponding to the maximum enhancement at 19 eV and the local minimum at 17.5 eV in the CIS plots. The spectra are normalized with respect to equal intensity at the high binding energy side which seems reasonable from the flux normalization of the superconductor spectra. The main valence band of the semiconducting sample is shifted about 0.25 eV towards higher binding energy as compared to the superconductor. The shift is consistent with the assumption that the introduction of potassium, apart from lattice distortions, mainly will cause a reduction of the band filling and, hence, a rigid band shift.²²

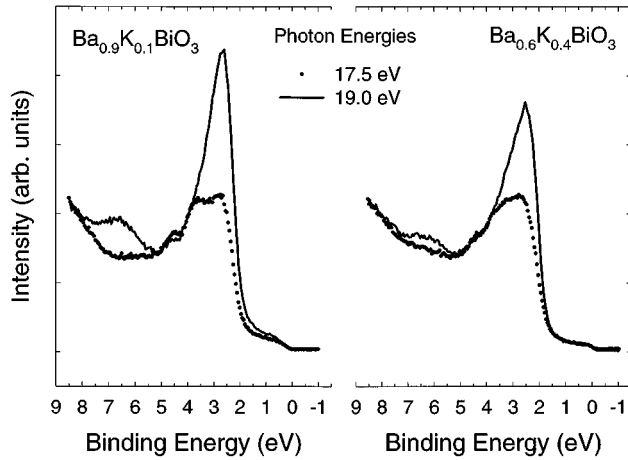


FIG. 5. A comparison of $\text{Ba}_{0.6}\text{K}_{0.4}\text{BiO}_3$ and $\text{Ba}_{0.9}\text{K}_{0.1}\text{BiO}_3$ valence-band photoemission spectra measured at photon energies 17.5 and 19 eV, corresponding to the off and on resonance, respectively. The spectra are normalized to equal intensity at the high binding energy side.

As seen in Fig. 5, the intensity enhancement at 2.6 and 6.3 eV E_b (with respect to the superconductor) and 19 eV PE is more pronounced in $\text{Ba}_{0.9}\text{K}_{0.1}\text{BiO}_3$ as compared to $\text{Ba}_{0.6}\text{K}_{0.4}\text{BiO}_3$. Since $\text{Ba}_{0.9}\text{K}_{0.1}\text{BiO}_3$ contains more Ba than $\text{Ba}_{0.6}\text{K}_{0.4}\text{BiO}_3$, the compositional relationship of the two compounds indicates that the valence-band enhancements at 19 eV PE could be Ba related. However, another explanation should also be considered. The more pronounced 19 eV PE resonance for $x=0.1$ could be related to the presence of more localized states in the semiconductor and a corresponding higher probability for a photoemission resonance. Further arguments for the Ba assignment of the valence-band enhancements will be given in the discussion below.

Resonant photoemission is a local probe because the feature which resonates is related to the element being core ionized in the absorption process which precedes the auto-ionization. This property makes it possible to obtain information about the partial DOS from valence-band photoemission resonances. For the present results, the pronounced inelastic background, especially at the lowest photon energies, makes it difficult to resolve the detailed behavior of the different features when the photon energy is changed. However, if the difference spectra 1–3 in Fig. 3 are considered, information regarding the partial DOS of the resonating features is obtained. The main similarity between the difference spectra 1 and 2 is that both spectra show a sharp peak at ~ 2.5 eV E_b , followed by an asymmetric tail towards the high binding-energy side. In the case of difference spectrum 3, the main peak is broader and much less intense than the others.

Since several shallow core levels (O 2s: $E_b=20$ eV, Ba 5p: $E_b=13$ and 15 eV, K 3p: $E_b=16$ eV) are located in the binding energy range of relevance when considering the excitation energies used for the spectra in Figs. 1 and 2, it is not straightforward to assign the partial DOS seen in the difference spectra to any of the constituents. However, by comparing the valence-band data at these low photon energies with spectra taken at thresholds of deeper core levels among the constituents, such an assignment may be possible. Because of the strong Ba 5p resonance seen at the 4d-4f

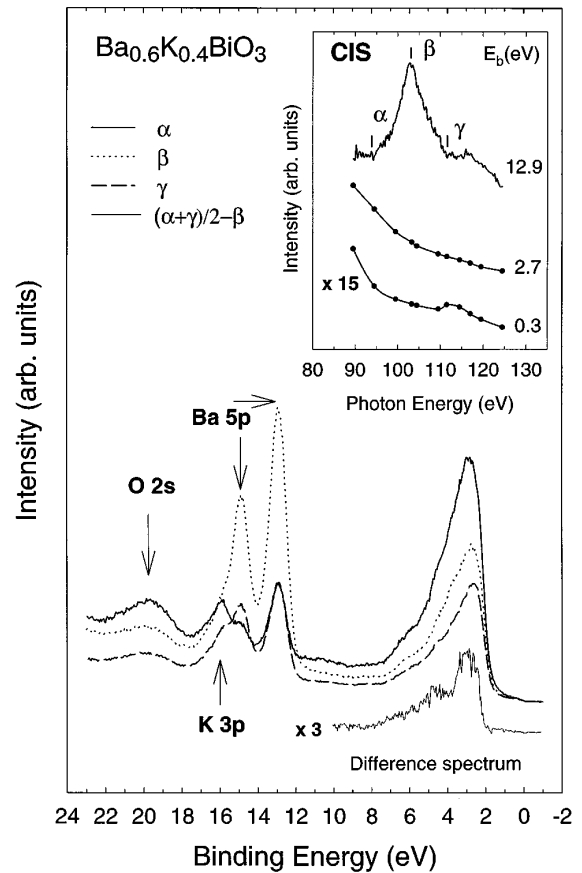


FIG. 6. CIS plots of $\text{Ba}_{0.6}\text{K}_{0.4}\text{BiO}_3$ around the Ba 4d absorption threshold. The top spectrum is measured directly at the Ba $5p_{3/2}$ peak, while the other two are extracted at $E_b=2.7$ and 0.3 eV, respectively, from a set of valence-band spectra normalized to the photon flux. Also shown are three valence-band spectra measured at the photon energies marked α , β , and γ in the CIS plot together with a calculated difference spectrum, as described in the text.

absorption threshold⁸ it is interesting to see whether the valence band also resonates at this threshold. In Fig. 6, CIS plots and selected spectra of Ba 5p and the valence band at the Ba 4d-4f threshold are shown for $\text{Ba}_{0.6}\text{K}_{0.4}\text{BiO}_3$. In the CIS plots, the 12.9 eV spectrum is recorded directly on the Ba $5p_{3/2}$ peak, while the 2.7 and 0.3 eV plots are extracted from a set of valence-band spectra with a binding energy window of 0.3 eV. The labels α , β , and γ in the CIS plot mark the photon energies used for the photoemission spectra shown in the figure. The maximum enhancement of Ba $5p_{3/2}$ is seen at 103.3 eV PE and has been attributed to a resonance involving a Ba 1P_1 intermediate state.⁸ The nature of the weaker structure at ~ 115 eV in the Ba 5p cross section has previously been discussed and it has been suggested that both a 4d and 5p core hole are involved in a double excitation to a $4d^9 5p^5 n l n' l$ (Refs. 23 and 24) intermediate state configuration decaying into a $5p^5$ final state. In the case of BaBiO_3 , Shen *et al.*⁸ have observed a decreased intensity in the valence band at the Ba 4d-4f threshold which was interpreted as an antiresonance. They extracted the Ba partial DOS from the valence band by using the technique of subtracting on antiresonance from off-antiresonance spectra. This partial DOS derivation did not take into account any photoemission cross section dependency of the dominating O

states in the valence band. However, applying a cross section compensated subtraction procedure at the Ba $4d-4f$ absorption threshold, similar to the one used for the low photon energy spectra (cf. Figs. 1–3), indicates that changes in the atomic cross sections cannot be neglected in this type of analysis. The difference spectrum is shown at the bottom of Fig. 6, denoted $(\alpha + \gamma)/2 - \beta$ (note the sign reversal due to the antiresonance as compared to the resonance effect in Figs. 2 and 3). Its shape is much narrower than the difference spectrum obtained by Shen *et al.*⁸ In fact, it is rather similar to difference spectrum 1 in Fig. 3 for the 16 eV resonance. The shape of the difference curve suggests that a Ba-related antiresonance occurs in the valence band since it differs from the general shape of the valence band. It is interesting to note that the difference spectrum at the Ba $4d$ threshold from Shen *et al.*⁸ looks rather similar to the difference spectrum 3 in Fig. 3 as well as to the general shape of the valence-band measured off-resonance.

To further support the notion of a weak antiresonance in the valence band at the Ba $4d-4f$ threshold rather than an atomic cross section effect, the shape of the extracted 2.7 eV CIS plot in Fig. 6 should be focused upon. Between 90 and 100 eV, this CIS curve shows a rather steep decrease in intensity followed by a smaller slope at higher energies. For a purely atomic cross-section-related phenomenon, a more continuous decrease in intensity could be expected.²⁵ Hence, as the intensity modulation occurs at the main 1P_1 absorption peak corresponding to a Ba $4d^9 6s^6 4f^1$, $\epsilon \ll 2$, intermediate state, we regard the difference spectrum in Fig. 6 to carry information concerning antiresonating Ba $6s^{\epsilon-1}$ final states.

Due to the similarities between the difference spectra in Fig. 3 and at the Ba $4d$ threshold in Fig. 6, we suggest the enhancements seen at 16 and 19 eV PE to be Ba derived. For the small enhancement at 22.5 eV PE the interpretation is less clear, although it could also be Ba related (cf. discussion below). These difference spectra, representing the spectral weight of barium in the main valence band, agrees well with the energy distribution of calculated Ba DOS from Mattheiss and Hamann⁴ by means of width and binding energy position.

From the CIS plot at $E_b = 0.3$ eV in Fig. 6, an intensity modulation is seen as a suppressed region around 100–110 eV, similar to the antiresonance in the main valence band, and an enhancement at 112–115 eV PE. The modulation is tentatively interpreted as a photoemission resonance, indicating Ba states close to the Fermi level. This result is not consistent with reported Ba partial DOS calculations of cubic BaBiO_3 ,⁵ nor ordered $\text{Ba}_{0.5}\text{K}_{0.5}\text{BiO}_3$,⁴ but in agreement with calculations made by Papaconstantopoulos *et al.*⁶ where Ba states are pronounced within 1 eV from E_F . On the other hand, this calculation predicts a much more narrow Ba DOS than observed and located around 4.3 eV binding energy, which is about 1.5 eV higher than calculations from Mattheiss and Hamann⁴ and the experimental results. In conclusion, none of the above calculations properly predicts the Ba partial DOS both with respect to the main energy distribution and contribution near the Fermi level, as compared to the experiments.

Since the binding energy of Ba $5p$ is located in close vicinity of the lowest photon energies used in the region

14–25 eV, the reasonable excitation energies for the possible Ba $5p-5d$ transitions have to be considered. Inverse photoemission measurements have shown a large density of empty Ba $5d$ states, located around 7 eV above the Fermi level,¹¹ which suggests excitation energies around 20 eV for possible Ba $5p-5d$ transitions. The actual lower photon energies (16 and 19 eV) for which the resonances are observed can be explained by a redistribution of empty states in the presence of a core hole. In this case, an interaction between the $5p$ hole and the $5d$ subshell lowers the energy of the $5d$ states²⁶ which makes the Ba $5p-5d$ transitions possible for photon energies less than 20 eV. Also, the calculated DOS from Mattheiss and Hamann⁴ predict Ba empty states from about 3 eV above the Fermi level which makes excitation energies below 20 eV possible.

In order to address this question, atomic calculations of the Ba $5p-5d$ transitions were performed utilizing the Cowan code²⁷ with relativistic corrections. From the dipole selection rules, three transitions from a $5p^6 6s^2 5d^0$ ground-state configuration to a $5p^5 6s^2 5d^1$ intermediate state are possible. The calculations show that the 1P_1 term at 23.0 eV is dominant compared to the 3D_1 term at 18.4 eV and the even weaker 3P_1 at 15.9 eV.²⁸ However, these calculations merely predict the excitation energies since hybridization makes the oscillation strengths unreliable.

In previously reported resonant photoemission results for atomic Ba, the expected $5p-5d$ giant dipole resonance (the 1P_1 intermediate state) has not been observed.^{29,30} This has been explained in terms of, e.g., Ba $5d-6s$ configuration mixing which results in a large number of $5p-5d$ dipole-allowed transitions obscuring the giant resonance behavior. According to these results, we do not expect the Ba 1P_1 term to be dominant in the absorption. Hence, the two resonances observed at 16 and 19 eV PE are, because of the good agreement with the atomic calculations, assigned to the Ba 3P_1 and 3D_1 intermediate states, respectively. In the case of the weak 22.5 eV PE resonance, it could possibly be assigned to any remnant of the Ba 1P_1 intermediate state.

It is also possible for the 22.5 eV resonance to be O related since the threshold energy is comparable to the O $2s$ binding energy. From inverse photoemission measurements, no clear O $2s-2p$ resonant enhancements have been seen¹¹ for $\text{Ba}_{1-x}\text{K}_x\text{BiO}_3$ in contrast to measurements done on cuprate superconductors.^{31,32} This indicates absence of localized O $2p$ holes in the $\text{Ba}_{1-x}\text{K}_x\text{BiO}_3$ system and that no strong O photoemission resonance could be expected as the O $2s-2p$ absorption threshold is tuned. However, the absence of a resonant enhancement in inverse photoemission does not exclude the possibility of having a weak enhancement in photoemission since the final states in the two experiments are different. This interpretation is consistent with the fact that the enhancement observed at 22.5 eV PE is very weak. The possibility that the 22.5 eV resonance is oxygen related is further supported by the fact that the corresponding difference spectrum (see Fig. 3) is broader than the difference spectra for 16 and 19 eV PE and resembles the valence band seen off-resonance, which is dominated by oxygen states.

IV. CONCLUSIONS

Resonant photoemission spectroscopy have been performed on $\text{Ba}_{1-x}\text{K}_x\text{BiO}_3$ single crystals with $x=0.1$ and x

≈ 0.4 in the photon energy range 14–25 eV. Resonant enhancements are seen in the valence band in the vicinity of the photon energies 16, 19, and 22.5 eV. By comparison with the valence-band antiresonance in the PE range 90–125 eV, i.e., at the Ba 4*d* threshold, the first two enhancements (16 and 19 eV PE) are suggested to originate from resonating Ba states at the threshold of the Ba 5*p*-5*d* transition. This interpretation is also supported by calculated atomic Ba 5*p*-5*d* dipole transition energies. The 22.5 eV feature is consistent both with such a Ba interpretation and an O resonance at the

O 2*s*-2*p* threshold. The results also indicate Ba states close to the Fermi level.

ACKNOWLEDGMENTS

This work was financially supported by the Swedish Research Council for Engineering Sciences, the Swedish Natural Science Research Council, the Royal Swedish Academy of Science, NEDO, and the Russian Scientific Council for high-temperature superconductor problems.

*Present address: INFM-Dip. di Fisica, Politecnico di Milano, Piazza L. Da Vinci 32, I-20133 Milano, Italy.

¹L. R. Mattheiss, E. M. Gyorgy, and D. W. Johnson, *Phys. Rev. B* **37**, 3745 (1988).

²L. F. Mattheiss and D. R. Hamann, *Phys. Rev. B* **28**, 4227 (1983).

³K. Takegahara and T. Kasuya, *J. Phys. Soc. Jpn.* **56**, 1478 (1987).

⁴L. F. Mattheiss and D. R. Hamann, *Phys. Rev. Lett.* **60**, 2681 (1988).

⁵N. Hamada, S. Massida, A. J. Freeman, and J. Redinger, *Phys. Rev. B* **40**, 4442 (1989).

⁶D. A. Papaconstantopoulos, A. Pasturel, J. P. Julien, and F. Cyrot-Lackmann, *Phys. Rev. B* **40**, 8844 (1989).

⁷A. Bansil and S. Kaprzyk, *Phys. Rev. B* **43**, 10 335 (1991).

⁸Z.-X. Shen, P. A. P. Lindberg, B. O. Wells, D. S. Dessau, A. Borg, I. Lindau, W. E. Spicer, W. P. Ellis, G. H. Kwei, K. C. Ott, J.-S. Kang, and J. W. Allen, *Phys. Rev. B* **40**, 6912 (1989).

⁹M. W. Ruckman, D. Di Marzio, Y. Jeon, G. Liang, J. Chen, M. Croft, and M. S. Hegde, *Phys. Rev. B* **39**, 7359 (1989).

¹⁰Y. Jeon, G. Liang, J. Chen, M. Croft, M. W. Ruckman, D. Di Marzio, and M. S. Hegde, *Phys. Rev. B* **41**, 4066 (1990).

¹¹T. J. Wagener, H. M. Meyer III, D. M. Hill, Yongyun Hu, M. B. Jost, J. H. Weaver, D. G. Hinks, B. Dabrowski, and D. R. Rich-ard, *Phys. Rev. B* **40**, 4532 (1989).

¹²M. Qvarford, V. G. Nazin, A. A. Zakharov, M. N. Mikheeva, J. N. Andersen, M. K.-J. Johansson, G. Chiaia, T. Rogelet, S. Söderholm, O. Tjernberg, H. Nylén, I. Lindau, R. Nyholm, U. O. Karlsson, S. N. Barilo, and S. V. Shiryaev, *Phys. Rev. B* **54**, 6700 (1996).

¹³Shiyong Pei, J. D. Jorgensen, B. Dabrowski, D. G. Hinks, D. R. Richards, A. W. Mitchell, J. M. Newsam, S. K. Sinha, D. Vaknin, and A. J. Jacobson, *Phys. Rev. B* **41**, 4126 (1990).

¹⁴S. L. Sorensen, B. J. Olsson, O. Widlund, S. Huldt, S.-E. Johanson, E. Källne, A. E. Nilsson, R. Hutton, U. Litzén, and A. Svensson, *Nucl. Instrum. Methods Phys. Res. A* **297**, 296 (1990).

¹⁵R. Nyholm, S. Svensson, J. Nordgren, and A. Flodström, *Nucl. Instrum. Methods Phys. Res. A* **246**, 267 (1986).

¹⁶J. N. Andersen, O. Björneholm, A. Sandell, R. Nyholm, J. Forsell, L. Thånell, A. Nilsson, and N. Mårtensson, *Synch. Rad. News* **4** (4), 15 (1991).

¹⁷R. B. Cairns and J. A. R. Samson, *J. Opt. Soc. Am.* **56**, 1568 (1966).

¹⁸M. Krumbrey, E. Tegeler, J. Barth, M. Krisch, F. Schäfers, and R. Wolf, *Appl. Opt.* **27**, 4336 (1988).

¹⁹Because of the interfering inelastic tail, the valence-band spectra

were also background subtracted before the difference spectra were obtained. This procedure did not alter the shape, nor the energy position of the peaked structure at 2.5 eV binding energy.

²⁰See for instance J. W. Allen, *Synchrotron Radiation Research*, edited by R. Z. Bachrach (Plenum, New York, 1992), p. 253.

²¹In angle-resolved photoemission, one must be cautious about polycrystalline properties of the surface. This could arise because of the sample fracturing (N.B. the surface is not macroscopically flat) and lead to a more angle-integrated picture in the spectra. In principle, if the spectra would reflect the angle-integrated DOS, the enhancements could be due to final-state effects instead of a photoemission resonance and the change of emission angle in Fig. 4 becomes meaningless for the investigation of the nature of the valence-band enhancements. However, we believe this is not the case since our normal emission valence-band data measured over a wide energy range (not included in this article) show signs of band-structure effects such as a band narrowing, probably corresponding to the Γ point.

²²Valence-band spectra in the photon energy range 14.5–25 eV were also measured for Ba_{0.9}K_{0.1}BiO₃. The general shape of these spectra were similar to the spectra for Ba_{0.6}K_{0.4}BiO₃ in Fig. 1.

²³G. Wendin, in *VUV Radiation Physics*, edited by E. E. Koch *et al.* (Vieweg-Pergamon, Berlin, 1974), p. 225.

²⁴M. H. Hecht and I. Lindau, *Phys. Rev. Lett.* **47**, 821 (1981).

²⁵The intensity deviation from the behavior of a polynomial of the third power (approximation of the photoionization cross section) can be fitted with a simple Fano profile with $q=0.1$ corresponding to an antiresonance. In this approach, the resulting CIS curve does not necessarily have to show a pronounced dip.

²⁶P. H. Kobrin, R. A. Rosenberg, U. Becker, S. Southworth, C. M. Truesdale, D. W. Lindle, G. Thornton, M. G. White, E. D. Poliakoff, and D. A. Shirley, *J. Phys. B* **16**, 4339 (1983).

²⁷R. D. Cowan, *The Theory of Atomic Structure and Spectra* (University of California Press, Berkeley, CA, 1981).

²⁸As Ba usually is assigned a +2 valency in solids, calculations were also performed for Ba III 5*p*⁶6*s*⁰. The calculated energies for the 5*p*-5*d* transitions were 24.4, 19.0, and 16.3 for the ¹P₁, ³D₁, and ³P₁ terms, respectively.

²⁹R. A. Rosenberg, M. G. White, G. Thornton, and D. A. Shirley, *Phys. Rev. Lett.* **43**, 1384 (1979).

³⁰J. P. Connerade and M. A. P. Martin, *J. Phys. B* **16**, L577 (1983).

³¹T. J. Wagener, Yongjun Hu, Y. Gao, M. B. Jost, J. H. Weaver, N. D. Spencer, and K. C. Goretti, *Phys. Rev. B* **39**, 2928 (1989).

³²H. M. Meyer III, T. J. Wagener, J. H. Weaver, and D. S. Ginley, *Phys. Rev. B* **39**, 7343 (1989).